Short Polymer Chain Statistics and the Relationship to End to End Electronic Excitation Transport: Random Walks with Variable Step Lengths

M. B. Zimmt,[†] K. A. Peterson, and M. D. Fayer*

Department of Chemistry, Stanford University, Stanford, California 94305.
Received July 8, 1987

ABSTRACT: The problem of the distribution of distances between the ends of a polymer chain for short chains (a small number of statistical segments) is considered. A formalism developed by Rayleigh is utilized to calculate the exact end to end distribution functions for random walks with a small number of steps and variable step lengths. In particular, distribution functions for walks in which the first and last step differ in length from the intervening steps are obtained. These are used as models for low molecular weight polymers in which the first and last statistical segments are different from internal segments because of chain end effects or chromophores attached to the chain termini. The results are used to calculate the ensemble averaged time dependence of end to end electronic excitation transport. $G^s(t)$, the part of the transport Green function which yields the time-dependent fluorescence depolarization observable, is calculated with exact random walk distribution functions and approximate distribution functions. It is demonstrated that the results are similar but that experiments which examine several distance ranges have the capability of distinguishing the distribution functions.

I. Introduction

Flory investigated various statistical mechanics models to describe the properties of chain molecules.[1] He concluded that a Gaussian spatial distribution function provides an adequate description of n-alkanes longer than 50–75 bonds. This class of polymers is modeled as freely jointed chains. Properties such as the distribution of end to end distances or the ensemble averaged root-mean-square radius of gyration can be obtained from the Gaussian description of the polymer chains. For any chain in which the directional correlation between bonds exists over a finite distance, the distribution function converges to a Gaussian expression in the limit of an infinitely long chain.

The Gaussian distribution function is a result of the application of the theory of random walks to the description of long freely jointed chain polymers.[2] For an ensemble of walkers executing random walks about an origin, the average spatial probability distribution of finding a walker a distance R from the origin for long walks is given by a Gaussian. In the polymer problem, the step size in the walk is the length of a statistical segment, i.e., the average distance required for the loss of directional correlation of the bonds in the polymer backbone.[3]

The Gaussian distribution function may not provide an accurate description of the spatial properties, for example, the end to end distance distribution, of short polymer chains (less than ten statistical segments). The equilibrium radial distribution function for the vector connecting the ends of a polymer chain is important to the description of the configurational statistics of chain molecules and for the interpretation of polymer properties, such as rubber

elasticity. The distribution of end to end distances for low molecular weight chains cannot be calculated by using the same Gaussian function (with appropriate changes for molecular weight) which accurately describes the end to end distances of high molecular weight chains. There are two reasons for this. First, short chains lack a sufficient number of statistical segments to achieve the Gaussian form. The distribution of end points for an ensemble of walks of N steps where N is a small integer is not accurately given by a Gaussian. In 1919, Rayleigh derived exact expressions for the end to end distribution functions of N step random walks ($N < 7$) of constant step size.[4] He also derived accurate approximations for the distribution function when N is larger. However, Flory pointed out that even if one properly employs the mathematics of short random walks to obtain the non-Gaussian description of the short wak, there can be a second problem. The freely jointed chain model ignores the perturbation introduced by chain end effects.[5] These effects are important for very short chains. They arise because the ends of a chain do not have the same configurational constraints as interior portions of the chain. An additional practical problem arises because many experimental approaches for the determination of end to end distribution functions employ polymers with molecular probes attached to the chain termini. The relevant quantity in these experiments is the probe-to-probe distance, which is identical with the polymer end to end distance only in the case of nonperturbing point probes.

For both short polymer chains and end-tagged polymers, a more appropriate description of the desired distribution function can be obtained with a freely jointed chain model employing two or more statistical segment (step) lengths: one representing the terminal chain segments and a second corresponding to the inner statistical segments. Such distribution functions enable consideration of both chain

[†] Permanent address: Chemistry Department, Brown University, Providence, RI 02912.

end and probe effects. This model is also relevant in investigations of block copolymer statistics.

In this paper, we derive exact end to end radial distribution functions for short freely jointed chains with nonidentical step lengths (nondegenerate chain). The method is based on the procedure employed by Rayleigh for identical step length short walks.[4] The most important results are the distribution functions given in eq 18 and 19. These equations permit the calculation of the probability of having an end to end distance, R, for any number of steps in a walk with variable step lengths. Each step in the walk can have a distinct length. Results are presented for two cases: walks with all steps of the same length and walks in which the first and last steps in the walk have a length which is distinct from the length of the other steps in the walk. The step lengths in the walks are taken to be the polymer chain statistical segment lengths. However, the statistical segment length is an average property. Even for the interior steps in a walk, there will be a distribution of step lengths. A variation in segment length could be incorporated by using eq 18 and 19 to average over an appropriate distribution function of segment lengths for each step in the walk. In the calculations presented below, for simplicity, we use the standard approach and replace the average over step sizes with the average step size, i.e., the statistical segment length.

The main focus of the calculations which are presented is to compare model end to end distribution functions for short chains (short walks) in which the first and last segments differ in length from the interior segments, with degenerate chain distribution functions and with the approximate Gaussian distribution function applied to short chains. It is found that in many situations, over a limited range of distances, the Gaussian distribution function, normally applied to long chains, is accurate, even for chains as short as three statistical segments. However, when a probe (tag) is attached to the chain ends, the choice of incorporating the extra length into the terminal chain segments or considering the tags as additional segments can be of crucial importance. The simple Gaussian approximation does not have the ability to incorporate the tags into a calculation in a reasonable manner.

To make the results more concrete, we calculate an electronic excitation transport observable for short chains.[6] The observable involves the time-dependent transfer of electronic excitation from a chromophore (tag) attached to one end of a chain to an identical chromophore attached to the other chain end. Electronic excitation transport is increasingly being used to investigate properties of polymer systems, particularly in solid polymer solutions where light scattering cannot be employed.[7] In addition, light scattering is not useful for the low molecular weight chains under consideration here. In an electronic excitation transport experiment, the tag at one end of the chain is optically excited at time $t = 0$. The electronic transition dipole–transition dipole interaction between the tags causes the excitation probability to redistribute between the two chromophores. (The concentration of tagged chains is taken to be low enough that excitation transfer between different chains is absent.) The function describing the decay of probability from the initially excited chromophore as a result of excitation transport is called $G^s(t)$.[8] $G^s(t)$ can be obtained experimentally from time-dependent fluorescence or absorption anisotropy measurements.[9]

It is straightforward to qualitatively understand the relationship between excitation transport dynamics and the end to end distribution function of an ensemble of isolated polymer chains which are end tagged with chromophores. An ensemble of tagged chains in a polymer blend or a viscous liquid solution will have a time-independent distribution of end to end distances. If the chains are of large size, the average distance between chromophores will be large relative to the distance scale over which excitation transport takes place. Since the rate of excitation transport depends on $1/R^6$ where R is the chromophore separation,[10] transport will be slow. For an ensemble of smaller end-tagged chains, the average chromophore separation will be less. This decrease in separation will result in more rapid excitation transport. The $1/R^6$ distance dependence makes the excitation transport observables very sensitive to small changes in end to end distribution function, and not just on the average separation, information about the distribution function can be obtained from an experimental determination of $G^s(t)$.[6b,9]

In time-resolved fluorescence depolarization experiments, a sample of randomly oriented chromophores is excited by a short pulse of polarized light. The initially excited ensemble is polarized along the direction of the excitation E field and gives rise to polarized fluorescence. The ensemble of excited states transfers excitation to ground-state chromophores with randomly oriented transition dipole moments. The ensemble of excited chromophores produced by excitation transfer gives rise to unpolarized fluorescence. The fluorescence from chains with short end to end distances is rapidly depolarized, whereas fluorescence from chains with large end to end separations is slowly depolarized. In principle, time-resolved fluorescence depolarization can be used as a direct probe of the distribution of end to end distances.

In section IV below, $G^s(t)$, the end to end excitation transport observable, is calculated by using the distribution functions derived in sections II and III. The differences between nondegenerate and degenerate short walk distribution functions and the Gaussian distribution function are illustrated. The effects of changing the length of the terminal segments are also discussed. It is found that in many instances, the differences between the distribution functions do not result in large changes in the observables. However, large differences are calculated for chains of identical total extended length if the tags are incorporated into the chain end segments as opposed to being taken as separate segments. By examining the distribution of end to end distances on several distance scales (using different end tag chromophores with different excitation transfer radii or examining the transfer for a single type of tag over a wide range of time scales), it should be possible to distinguish among model distribution functions. Although the differences in the calculated curves are not large, they are comparable to those measured in polymer excitation transport experiments previously reported for chains that are randomly tagged as opposed to end tagged.[9a]

II. Theoretical Development

The distribution of end to end distances for an ensemble of polymer chains is described by the radial distribution function. We want to derive the distribution function for a polymer chain with nonconstant statistical segment lengths. The polymer chain is modeled as a three-dimensional random walk in which each step may be a different length; the step lengths in the walk correspond to the statistical segments of the polymer chain. Rayleigh prescribed a method to obtain exact solutions for the radial distribution function of an N-step random walk in three dimensions.[4] We follow essentially the derivation of Rayleigh with three important differences. (1) We employ Fourier transform methods to obtain the integral form of

the radial distribution function (eq 5). (2) We maintain independent step lengths throughout the calculation (a nondegenerate random walk). (3) We derive an exact expression for the end to end radial distribution function for random walks (polymer chains) of arbitrary step number and step length.

The radial distribution function for the random walk depends on the probability distribution of the individual steps. Modeling the polymer chain as a string of statistical segments removes angular dependences between steps of the walk. The probability distribution[11] for step j of length l_j is

$$p_j(\vec{r}) = \frac{1}{4\pi l_j^2} \delta(|\vec{r}| - l_j) \quad (1)$$

$\vec{r}$ is the vector representing the step. The characteristic function of step j, Λ_j, is defined as the Fourier transform of the probability distribution.[11]

$$\Lambda_j(\hat{\omega}) = \int_{-\infty}^{\infty} e^{i\hat{\omega}\cdot\vec{r}} p_j(\vec{r}) \, d\vec{r} \quad (2)$$

The end to end distribution function, $\rho_N(R)$, of the N-step random walk is the inverse Fourier transform of the product of the characteristic functions of the individual steps.[11] In three dimensions, the density distribution function for the end to end vector $\mathbf{R}$ is formally written as

$$\rho_N(\vec{R}) = \frac{1}{(2\pi)^3} \int_{-\infty}^{\infty} e^{-i\hat{\omega}\cdot\vec{R}} \left\{ \prod_{j=1}^{N} \Lambda_j(\hat{\omega}) \right\} d\hat{\omega} \quad (3)$$

Substitution of eq 1 and 2 into eq 3 and integration yields

$$\rho_N(\vec{R}) = \frac{1}{2\pi^2 R} \int_0^{\infty} \omega \sin(\omega R) \prod_{j=1}^{N} \left(\frac{\sin \omega l_j}{\omega l_j} \right) d\omega \quad (4)$$

The integral form of the end to end radial distribution function, $P_N(R)$, is easily obtained.

$$P_N(R) = 4\pi R^2 \rho_N(\vec{R}) =$$
$$\frac{2R}{\pi} \int_0^{\infty} \omega \sin(\omega R) \prod_{j=1}^{N} \left(\frac{\sin \omega l_j}{\omega l_j} \right) d\omega \quad (5)$$

The end to end radial distribution function (RDF) for an ensemble of polymer chains is given by eq 5. R is the end to end distance of the chain, and l_j is the length of the jth statistical segment in the polymer chain. $P_N(R)$ is independent of the order of connectivity of the statistical segments. This is a consequence of modeling the chain as a random walk with no angular correlations between steps.

The form of the solution to eq 5 depends on the number of steps in the walk. We are interested in the RDFs of short polymer chains that contain a small number of statistical segments (steps in the walk). The solutions for the cases $N = 1$ or 2 were provided by Rayleigh.

$$P_1(R) = \delta(R - l_1) \quad (6)$$
$$P_2(R) = R/(2l_1l_2) \quad (7)$$

The result for $N = 1$ is obvious. For $N = 2$, the radial distribution function increases linearly from $R = |l_1 - l_2|$, the shortest possible end to end distance, up to $R = l_1 + l_2$, the fully extended chain length.

The solution of eq 5 for the three-step random walk is the basis for the solution of all longer walks. The integral is evaluated by recasting into a sum of terms of the form

$$\int_0^{\infty} \frac{\sin^2 a\omega}{\omega^2} \, d\omega = \frac{\pi}{2} |a|$$

To achieve this form, eq 5 is rewritten as

$$\frac{P_3(R)}{R} = \frac{2/\pi}{l_1 l_2 l_3} \int_0^{\infty} \frac{\sin(\omega R)}{\omega^2} \prod_{j=1}^{3} \sin(\omega l_j) \, d\omega =$$
$$\frac{2/\pi}{l_1 l_2 l_3} \int_0^{\infty} I_3(\omega) \, d\omega \quad (8)$$

The integrand product, $I_3(\omega)$, is expanded into a sum of eight cosine functions. (For an N-step walk the expansion produces 2^N cosine functions.)

$$I_3(\omega) = \sum_{\beta_1=0}^{1} \sum_{\beta_2=0}^{1} \sum_{\beta_3=0}^{1} \frac{(-1)^{\beta_1+\beta_2+\beta_3}}{2^3} \cos\left[\omega(R - \sum_{i=1}^{3}(-1)^{\beta_i}l_i)\right] \quad (9)$$

The cosine terms are replaced by using the half angle formula, $\cos(2x) = (1 - 2\sin^2(x))$. The constants cancel as there are equal numbers of positive and negative terms in the summations in eq 9.

$$\frac{P_3(R)}{R} = \frac{2/\pi}{l_1 l_2 l_3} \int_0^{\infty} d\omega \sum_{\beta_1=0}^{1} \sum_{\beta_2=0}^{1} \sum_{\beta_3=0}^{1} \frac{(-1)^{\beta_1+\beta_2+\beta_3}}{2^3} \times$$
$$\left[\frac{2 \sin^2\left[\frac{\omega}{2}(R - \sum_{i=1}^{3}(-1)^{\beta_i}l_i)\right]}{\omega^2} \right] \quad (10)$$

Integration yields the radial distribution function, $P_3(R)$.

$$P_3(R) = \frac{2^{-3}R}{l_1 l_2 l_3} \sum_{\beta_1=0}^{1} \sum_{\beta_2=0}^{1} \sum_{\beta_3=0}^{1} (-1)^{\beta_1+\beta_2+\beta_3}[|R - \sum_{i=1}^{3}(-1)^{\beta_i}l_i|] \quad (11)$$

Equation 11 for $P_3(R)$ is zero at $R = 0$ and at $R = l_1 + l_2 + l_3$. When all step lengths are equal, eq 11 reduces to Rayleigh's solution for a degenerate three step walk.

To determine the radial distribution functions of walks longer than three steps, eq 5 is divided by R and is differentiated, with respect to R, $N - 3$ times.[4] This recovers the form of the integrand present in eq 8.

$$N \text{ odd}$$

$$\frac{d^{N-3}(P_N(R)/R)}{dR^{N-3}} =$$
$$\frac{2/\pi}{\prod_{j=1}^{N} l_j} (-1)^{(N+1)/2} \int_0^{\infty} \frac{\sin(\omega R)}{\omega^2} \prod_{j=1}^{N} \sin(\omega l_j) \, d\omega \quad (12)$$

$$N \text{ even}$$

$$\frac{d^{N-3}(P_N(R)/R)}{dR^{N-3}} =$$
$$\frac{2/\pi}{\prod_{j=1}^{N} l_j} (-1)^{N/2} \int_0^{\infty} \frac{\cos(\omega R)}{\omega^2} \prod_{j=1}^{N} \sin(\omega l_j) \, d\omega \quad (13)$$

Trigonometric substitution and integration in the same manner as performed for $N = 3$ yields equations for the $N - 3$ derivative of $P_N(R)/R$.

$$\frac{d^{N-3}(P_N(R)/R)}{dR^{N-3}} = \frac{(-1)^{N+1}2^{-N}}{\prod_{j=1}^{N} l_j} \sum_{\{\beta_j\}=0}^{1} (-1)^{\sum \beta_j}\{|R - R_\Delta(\{\beta_j\})|\} \quad (14)$$

$$R_\Delta(\{\beta_j\}) = \sum_{j=1}^{N} (-1)^{\beta_j} l_j \quad (15)$$

$\{\beta_j\}$ is a set of N indices which independently assume the

values 0 and 1. The summation in eq 14 is an N-tuple sum over the N elements of $\{\beta_j\}$, and it contains 2^N terms. For example, eq 11 for the three-step walk ($N = 3$) contains eight (2^3) terms originating from the three independent summations over the set $\{\beta_j\} = \{\beta_1,\beta_2,\beta_3\}$. The factor $(-1)^{N+1}$ in eq 14 accounts for N odd or even. The value of $R_\Delta(\{\beta_j\})$ is different in each of the 2^N terms of the N-tuple sum and must be reevaluated for each term according to eq 15.

The radial distribution function is recovered by integrating eq 14 $N - 3$ times, subject to the boundary condition that all derivatives of the distribution function must vanish at the fully extended chain length,[4] i.e.

$$\frac{\mathrm{d}^x(P_N(R)/R)}{\mathrm{d}R^x} = 0 \quad \text{at} \quad R = R_\mathrm{m} = \sum_{i=1}^{N} l_i \qquad (16)$$

Integration of the absolute value terms in the summation in eq 14 and application of the boundary conditions (eq 16) yields

$$\frac{\mathrm{d}^{N-4}(P_N(R)/R)}{\mathrm{d}R^{N-4}} =$$
$$\frac{(-1)^{N+1}}{2} \frac{2^{-N}}{\prod\limits_{i=1}^{N} l_i} \sum_{\{\beta_j\}=0}^{1} (-1)^{\Sigma\beta_i}[|R - R_\Delta|(R - R_\Delta) - (R_\mathrm{m} - R_\Delta)^2]$$

$$(17)$$

$R_\Delta \equiv R_\Delta(\{\beta_i\})$. The term $-(R_\mathrm{m} - R_\Delta)^2$ arises from application of the boundary conditions. Integration and application of the boundary conditions $N - 4$ times more generates the radial distribution functions.

N odd

$$P_N(R) = \frac{2^{-N}R}{(N - 2)!\prod\limits_{i=1}^{N} l_i} \sum_{\{\beta_j\}=0}^{1} (-1)^{\Sigma\beta_i}\Bigg[|R - R_\Delta|^{N-2} +$$
$$\left\{ \sum_{i=0}^{N-5} \binom{N-2}{i+1}(-1)^i(R_\mathrm{m} - R)^{i+1}(R_\mathrm{m} - R_\Delta)^{N-i-3} \right\} -$$
$$(R_\mathrm{m} - R_\Delta)^{N-2} \Bigg] \quad (18)$$

N even

$$P_N(R) =$$
$$\frac{2^{-N}R}{(N - 2)!\prod\limits_{i=1}^{N} l_i} \sum_{\{\beta_j\}=0}^{1} (-1)^{\Sigma\beta_i}\Bigg[|R - R_\Delta|^{N-3}(R - R_\Delta) +$$
$$\left\{ \sum_{i=0}^{N-5} \binom{N-2}{i+1}(-1)^i(R_\mathrm{m} - R)^{i+1}(R_\mathrm{m} - R_\Delta)^{N-i-3} \right\} -$$
$$(R_\mathrm{m} - R_\Delta)^{N-2} \Bigg] \quad (19)$$

For $N = 4$–7 and constant step lengths, $l_j = l$, eq 18 and 19 are identical to Rayleigh's solutions. Equations 11, 18, and 19 are exact expressions for the radial distribution functions of random walk models of polymer chains comprising three or more statistical segments. RDFs of polymer chains modeled as degenerate walks are obtained by setting all step lengths equal. Block copolymer RDFs can be modeled by employing the number and lengths of statistical segments appropriate to each homopolymer component. We are particularly interested in the RDFs of low molecular weight polymers with fluorescent chromophores (tags) attached at both chain termini. The time dependence of energy transfer observables depend on the distance of separation of the tags, which is identical with
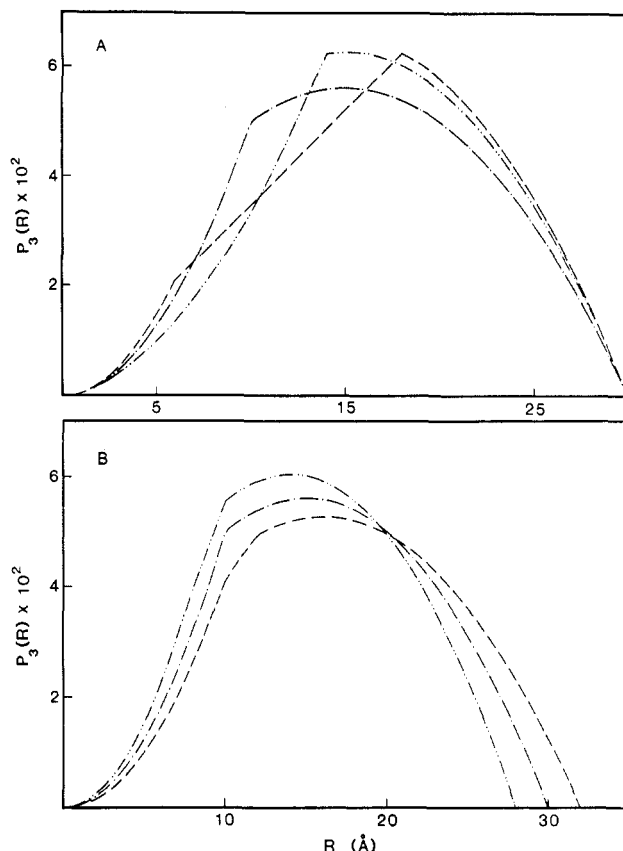
Figure 1. Exact radial distribution functions, $P_3(R)$, for three-segment polymer chains containing two identical terminal statistical segments l_T and one internal statistical segment l. (A) The chains have the same extended length of 30 Å; $l_\mathrm{T} = 12$ Å, $l = 6$ Å (———); $l_\mathrm{T} = 10$ Å, $l = 10$ Å (·——·); $l_\mathrm{T} = 8$ Å, $l = 14$ Å (—··—). (B) Chain end effects and end tagging are modeled by shortening and lengthening, respectively, the terminal segments; $l_\mathrm{T} = 9$ Å, $l = 10$ Å (—··—); $l_\mathrm{T} = 10$ Å, $l = 10$ Å (·—··); $l_\mathrm{T} = 11$ Å, $l = 10$ Å (———).

the polymer chain end to end separation only for the case of point chromophores. The tag to tag RDF can be calculated by using two statistical segment lengths; one representing the inner, homopolymer, statistical segments and a second representing the terminal chain segments plus tag.
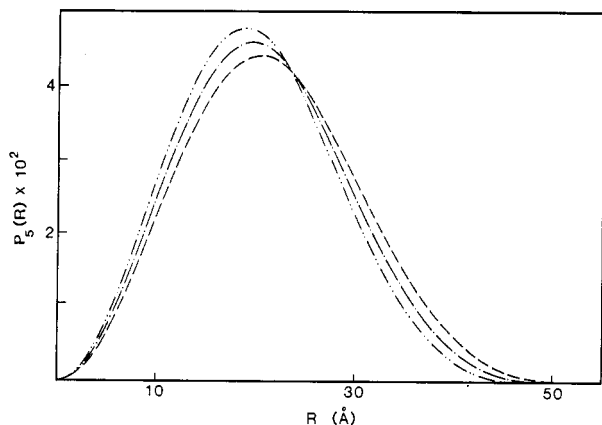
III. Calculated Radial Distribution Functions

Calculations of the RDF for freely jointed chains comprising three to five statistical segments are presented in Figures 1–4. The exact distribution functions, derived above, for random walk models of polymer chains comprised of one (degenerate) and two (nondegenerate) statistical segment lengths are shown as broken curves. Gaussian RDFs[1] (eq 20), appropriate in the limit of long chains of a single statistical segment length, are shown as solid curves,

$$P_N^G(R) =$$
$$\left(\frac{3}{2\pi\langle R_\mathrm{ee}^2\rangle_0} \right)^{3/2} \exp(-3R^2/2\langle R_\mathrm{ee}^2\rangle_0)R^2 \quad \langle R_\mathrm{ee}^2\rangle_0 = Nl^2$$

$$(20)$$

where $\langle R_\mathrm{ee}^2\rangle^{1/2}$ is the root-mean-square end to end distance. In the figures, a statistical segment length of 10 Å is employed unless otherwise stated.

Exact RDFs for three-segment degenerate ($3l$) and nondegenerate ($2l_\mathrm{T}, l$) chains of constant extended length are displayed in Figure 1A. l_T is the terminal segment
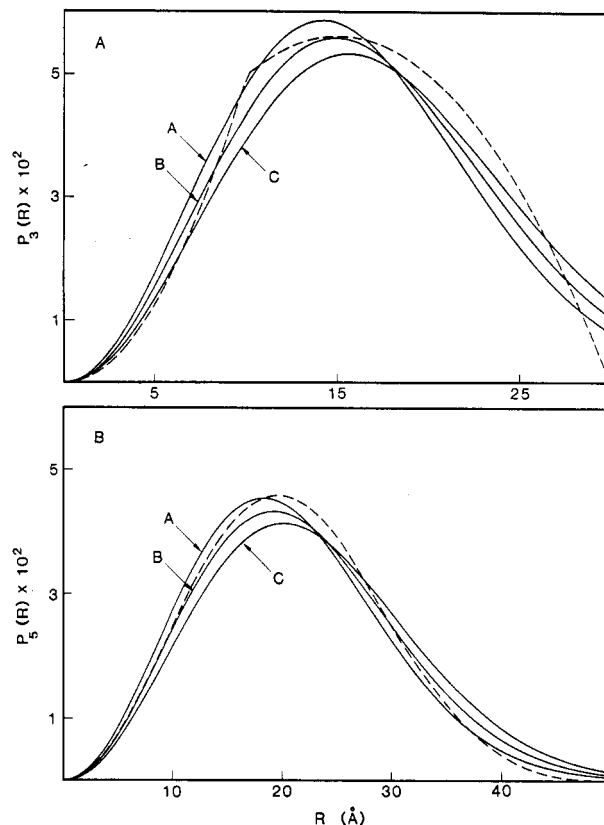
Figure 2. Exact radial distribution functions, $P_5(R)$, for five-segment polymer chains containing two identical terminal statistical segments l_T and three identical internal statistical segments, l = 10 Å. Chain end effects and end tagging are modeled by shortening and lengthening, respectively, the terminal segments; l_T = 9 Å (— · ·); l_T = 10 Å (· — ·); l_T = 11 Å (——).
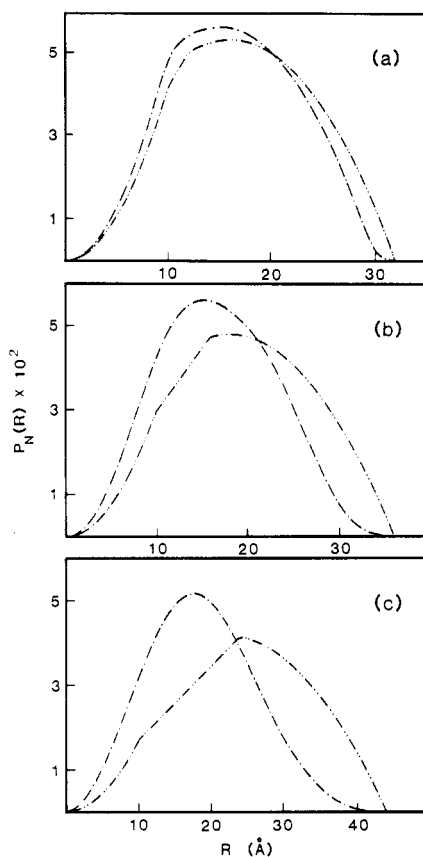
Figure 3. Radial distribution functions calculated for two models of end tagged polymer chains. The untagged polymer chains contain three 10-Å statistical segments. The tags are either incorporated into the terminal segments (N = 3) or added as two additional segments (N = 5). (a) Tag = 1 Å: l_T = 11 Å, $P_3(R)$ (— · ·); l_T = 1 Å, $P_5(R)$ (· — ·). (b) tag = 5 Å: l_T = 15 Å, $P_3(R)$ (· — ·); l_T = 5 Å, $P_5(R)$ (· — ·). (c) tag = 7 Å: l_T = 17 Å, $P_3(R)$ (— · ·); l_T = 7 Å, $P_5(R)$ (· — ·).

length. l is the internal segment length. The most probable end to end distance and the moments of the exact distribution function increase as the step lengths are made dissimilar. The most compact distribution for a chain of fixed extended length and number of steps is that of the degenerate chain.

As noted by Rayleigh, $P_3(R)$ does not have a continuous first derivative. $P_3(R)$ exhibits cusps at R equal to the smaller of l and l_T and at the larger of $2l_T - l$ and l. The

Figure 4. Exact and Gaussian radial distribution functions calculated for polymer chains containing three identical statistical segments (A) or five identical statistical segments (B). The Gaussian RDFs are drawn as solid lines: (A) $P_3(R)$, l_T = l = 10 Å (——); $P_3{}^G(R)$, l_{EF} = 10 Å (A); $P_3{}^G(R)$, l_{EF} = 10.5 Å (B); $P_3{}^G(R)$, l_{EF} = 11 Å (C); (B) $P_5(R)$, l_T = l = 10 Å (——); $P_5{}^G(R)$, l_{EF} = 10 Å (A); $P_5{}^G(R)$, l_{EF} = 10.5 Å (B); $P_5{}^G(R)$, l_{EF} = 11 Å (C).

appearance of the cusps is a consequence of using a single value for the length of each step. In an actual polymer system, variations in step length (segment length) about some average will wash out cusps and other features on distance scales on the order of or smaller than one segment length. It is important to note that in all of the calculations presented here, a single fixed length is used for each step in the walk. However, the general formalism presented in section II can be used for any sequence of step lengths. Therefore it would be straightforward to average over a distribution of lengths for each step in a walk. Such a procedure would smooth out the cusps which appear in Figures 1, parts A and B, 3, and 4A but will leave the shapes of the curves essentially unchanged.

In the proximity of chain termini, the equilibrium fraction of gauche bond rotational states is higher than in the chain interior. This effect is unimportant after the fourth bond from the terminus in polymethylene.[5] The larger gauche content near the chain termini produces a small decrease in the average chain dimensions. This effect can be modeled by using a terminal statistical segment length smaller than the normal, interior, statistical segment length.

Chromophores attached to chain termini increase the end to end length of the chain. The chromophores can be incorporated into the model chain by increasing the terminal statistical segment lengths. RDFs of three-segment chains with terminal segments shortened or lengthened by 10% are displayed in Figure 1B. The decreased terminal segment length is a model for the chain end effects described above. The increased terminal segment length is one possible model for the inclusion of end tags. Figure

1B displays how these considerations affect the RDF. Increasing the terminal segment lengths extends the range of chain end to end distances and shifts the most probable end to end distance to longer R. Scaling the RDFs displayed in Figure 1B as $P_3(R)/P_3(\text{max})$ versus $R/\sum l_i$ generates curves that are superimposable except in the regions between the cusps. ($P_3(\text{max})$ is the maximum value of a given RDF.) Changing the terminal segment lengths by 10% has little effect on the qualitative shape of $P_3(R)$. The qualitative shape of the RDF determines the form of calculated time-dependent observables. Therefore, it will be possible to fit the experimental observable by making small changes in the statistical parameters of either of these RDF models. The different RDF models will yield slightly different statistical parameters.

Longer polymer chains have more internal statistical segments and should be less sensitive to changes in the terminal segment lengths. RDFs of polymers with five statistical segments and various terminal segment lengths are shown in Figure 2. $P_5(R)$ broadens and the maximum shifts to larger R as the terminal segment lengths are increased. When replotted as $P_5(R)/P_5(\text{max})$ versus $R/\sum l_i$, the RDFs are superimposable. The shifts in the most probable end to end distances accompanying the 10% changes in the terminal segment lengths amount to 1 Å for $P_3(R)$ (Figure 1B) and 0.75 Å for $P_5(R)$ (Figure 2).

Small increases in the terminal segment lengths shift and broaden the radial distribution functions. Larger changes in the terminal segment lengths produce more drastic changes in the RDF shape, particularly in $P_3(R)$. Polymers with long and/or flexible end-tagged chromophore units may also be modeled by adding two statistical segments, corresponding to the tags, to the N statistical segments comprising the polymer chain. The choice of model for the end-tagged chain is important. However, knowledge of the molecular structure of the tag can remove some of the uncertainty. Very flexible end tags are probably best modeled as independent segments, while rigid tags should probably be included as part of the chain terminal segments.

Increasing the number of segments in a chain of constant extended length shifts probability in the RDF to smaller end to end distances. Figure 3 shows comparisons of three- and five-step nondegenerate RDFs in which end tags of length 1, 3, or 7 Å have been added to a polymer chain consisting of three 10-Å statistical segments. The tags have either been added to the terminal segments ($P_3(R)$) or added as terminal segments ($P_5(R)$).[12] With 1-Å tags (Figure 3A) the difference between the three- and five-step RDFs is comparable to the difference between a degenerate three-step RDF and the Gaussian RDF with the same root mean square end to end distance (vide infra, see Figure 4A). The motivation for use of the exact RDF is that it more accurately reflects the statistics of the ensemble of polymer chains. If added tags are not properly modeled, however, the tagging experiment may lead to as much ambiguity in the statistical parameters as would the use of a Gaussian RDF. With tags of 3 or 7 Å (Figure 3, parts B and C) the bulk of the probability distribution in the three-step RDF is shifted to distances 5–10 Å longer than in the five-step RDF. As we will demonstrate below, differences of this magnitude in RDFs are detectable in both calculated and experimental observables.

Gaussian radial distribution functions (eq 20) are often used to model the end to end statistics of polymer chains. The Gaussian description is only valid for long random walks, but, due to its simplicity, is often used to model short and intermediate length polymer chains. As previously noted by Flory,[1] the degenerate RDFs, $P_N(R)$, are roughly approximated by using Gaussian RDFs, $P_N{}^G(R)$, even for $N = 3$. The most probable end to end distance of a Gaussian RDF (N steps of length l) is smaller than that of the degenerate exact RDF (Figure 4). The second moments of the Gaussian and degenerate chain RDFs are identical. This is an artifact of the Gaussian RDF exhibiting substantial probability at distances greater than the fully extended chain length.

Figure 4, parts A and B, show qualitative similarities between the exact degenerate and Gaussian RDFs calculated for identical segment lengths. The correspondence improves as N increases and is almost perfect for $N = 20$.[1] Over limited ranges of the end to end distance R, the degenerate exact RDF may be more closely approximated by using a Gaussian RDF with an "effective" statistical segment length, l_{EF}, that is longer than the actual segment length. For $l = 10$ Å and $R < 8$ Å, the degenerate RDF $P_3(R)$ is best approximated by $P_3{}^G(R)$ with $l_{EF} = 11$ Å (Figure 4A). For $R < 15$ Å, $P_3{}^G(R)$ with $l_{EF} = 10.5$ Å mimics $P_3(R)$ more accurately than with $l_{EF} = 10$ Å. $P_5(R)$ is nearly identical with $P_5{}^G(R)$ with $l_{EF} = 10.5$ Å for $R < 13$ Å (Figure 4B).

The congruence induced between the different RDF forms over limited end to end distance ranges by use of effective statistical segment lengths is very important with regard to experimental investigations of polymer statistics. The end to end RDF describing an ensemble of polymer chains cannot be directly determined in an experiment. Evidence for a specific form of the RDF lies in successful simulation of experimental observables: statistical parameters of the RDF are varied to obtain the best fit between calculated and experimental results. As shown above, RDFs with distinct forms can be made to appear similar over limited distance ranges. Experimental observables, dependent on the probability distribution of chains only within this end to end distance range, cannot be used to distinguish between the various forms of the polymer RDF. Use of experimentally determined parameters and the RDF form outside the distance range probed by the experiment could be entirely unwarranted. For example, compare the behavior of $P_3(R)$ ($l = 10$ Å) and $P_3{}^G(R)$ ($l_{EF} = 11$ Å) for $R > 9$ Å (Figure 4A). Calculated observables sensitive to the RDFs at long distances will appear dramatically different when using these two RDFs, while calculated observables sensitive to the RDF only for $R < 9$ Å will appear identical.

To unambiguously establish the functional form and parameters of the RDF describing an ensemble of polymer chains, it is necessary to employ an observable which is sensitive to the RDF throughout the range of extension of the polymer chain. Alternatively, one can perform a series of experiments, each of which is sensitive over a different fraction of the accessible end to end distance range.

In the next section, we describe the application of electronic excitation transport experiments to the investigation of polymer end to end chain statistics. Excitation transport rates decrease rapidly as chromophore separation is increased. This causes the transport observable to be sensitive to the short distance portion of the radial distribution function. We calculate the electronic excitation transport observable for isolated polymer chains end tagged with chromophores, using Gaussian and exact models of the end to end RDF. The results show that using a series of chromophore pairs, which undergo excitation transfer over different distance ranges accessible to the polymer chain or measuring the time dependence of

the excitation transport over a wide range of time scales, can provide a test for the form of the radial distribution function.

IV. Electronic Excitation Transport

Consider an ensemble of randomly configured polymer chains in solid solution that are substituted at both termini with identical chromophores (tags). The concentration of tagged chains is sufficiently low that there is no interaction between chromophores on different chains. At $t = 0$, the tag at one chain end is excited. Transition dipole–transition dipole interactions between the two chromophores cause the excitation probability on the initially excited tag to decay and the probability on the other tag to increase. In excitation transport studies, the quantity of experimental and theoretical interest, $G^s(t)$, is the ensemble average probability that the initially excited chromophore is still excited at time t later.[6b–c,8,9] Throughout the following discussion, $G^s(t)$ includes only the loss of probability due to excitation transport. To include probability loss from excited-state decay, $G^s(t)$ must be multiplied by $\exp(-t/\tau)$.[6c]

For an ensemble of isolated end-tagged chains, $G^s(t)$ is given by[6c]

$$G^s(t) = \int_0^\infty P_N(R) \frac{[1 + e^{-2\omega(R)t}]}{2} \, dR \qquad (21)$$

$\omega(R)$ is Forster's expression for the rate of dipole–dipole induced excitation transport.[10]

$$\omega(R) = \frac{1}{\tau}\left(\frac{R_0}{R}\right)^6 \qquad (22)$$

R is the chromophore separation. τ is the excited state lifetime. R_0 is the Forster critical transfer radius and is a property of the specific chromophore pair employed. Equation 22 is the orientation averaged expression for dipole–dipole interactions and is applicable to rapidly rotating chromophores. For the systems of interest in this paper, the chromophores are essentially static. In order to account for static dipole–dipole angular factors, R_0 in eq 22 must be replaced by[13]

$$R'_0 = (\gamma_2)^{1/3}R_0 \qquad \gamma_2 = 0.8468$$

Polymer chains in which the chromophores are separated by $R = R_0$ undergo excitation transport and excited-state decay at similar rates. Excitation transport occurs much more rapidly in polymer chains with $R < R_0$. Chains with $R \gg R_0$ undergo little excitation transport during the excited-state lifetime. Accurate experimental determination of $G^s(t)$ is difficult for $t > 3\tau$ due to excited-state decay. For $t < 3\tau$, excitation transport occurs to less than 10% for chains with end to end distances $R > 2R_0$. Consequently, experimental determination of $G^s(t)$ can be used to examine $P_N(R)$ in the range $R < 2R_0$.

If a sample of randomly oriented chromophores is excited by a short pulse of plane-polarized light, the decay of the fluorescence intensities polarized parallel, $I_\parallel(t)$, and perpendicular, $I_\perp(t)$, to the direction of the E field of the excited light can be written as[9a]

$$I_\parallel(t) = e^{-t/\tau}(1 + 2r(t))$$

$$I_\perp(t) = e^{-t/\tau}(1 - r(t)) \qquad (23)$$

$r(t)$ is the fluorescence anisotropy. It contains information about all sources of depolarization and is experimentally obtained from

$$r(t) = \frac{I_\parallel(t) - I_\perp(t)}{I_\parallel(t) + 2I_\perp(t)} \qquad (24)$$

If the transition dipoles of the tags in the polymer matrix are randomly oriented, the major source of depolarization is excitation transport. Slow depolarization due to chromophore motion can be treated as previously described.[9a] $G^s(t)$ is obtained from $r(t)$ by dividing $r(t)$ obtained experimentally from a sample with two tagged ends by $r(t)$ from a sample lacking energy transport, for example, a one end-tagged polymer or a doubly end-tagged polymer with end to end distances so great that excitation transport does not occur to any measurable extent. This procedure removes inherent and rotational depolarization effects.

The initially excited ensemble is polarized along the direction of the excitation E field and gives rise to polarized fluorescence. The chromophores on the chain termini are on different statistical segments, so there is no correlation between the directions of their transition dipole moments. Intrachain excitation transfer to the initially unexcited chromophore and subsequent emission results in depolarization of the fluorescence. At equilibrium, the probability of locating the excitation on either tag is 0.50. [Experimentally, there will be a small amount of residual polarization ($\sim$4%) in the fluorescence anisotropy of the initially unexcited tags.[14] This can usually be neglected.] Experimental $G^s(t)$ attains $\sim$0.5 for $t < 3\tau$ only if the Forster transfer radius is larger than the fully extended chain length.

For the subset of chains with a given end to end distance R, eq 22 gives the rate, or more importantly, the time scale [0 to $1/\omega(R)$] during which substantial excitation transport and concomitant fluorescence depolarization occur. The radial distribution function determines the fraction of polymer chains with this end to end separation and thereby controls the amount of depolarization and the decrease of $G^s(t)$ occurring during this time range.

Alternatively, at time t_1, all tagged chains with end to end distance less than $R_1 = (2t_1/\tau)^{1/6}R_0$ have undergone substantial excitation transfer. The fluorescence derived from these chains exhibits the equilibrium anisotropy. The decrease of $G^s(t)$ prior to $t = t_1$ is related to the integrated probability in $P_N(R)$ between 0 and R_1.

In Figure 5, we present $G^s(t)$ curves calculated with degenerate exact and Gaussian RDFs for polymer chains with three statistical segments (Figure 5A) and four statistical segments (Figure 5B). We employ the following notation. $G^s_G(t;l_{EF},R_0)$ is $G^s(t)$ calculated by using the Gaussian RDF with an effective statistical segment length, l_{EF}, and a Forster transfer radius R_0. $G^s_E(t;l_T,l,R_0)$ is $G^s(t)$ calculated by using the exact RDF with terminal statistical segment lengths, l_T, internal segment lengths, l, and a Forster transfer radius, R_0.

In Figure 5A, $R_0 = 10$ Å. For $t < 0.3\tau$, $G^s_G(t;11,10)$ and $G^s_E(t;10,10,10)$ exhibit similar time dependences. At short distances the corresponding RDFs are in close agreement. However, for $0.6\tau < t < 3\tau$, $G^s_G(t,10.5,10)$ with $l_{EF} = 10.5$ Å is in much better agreement with $G^s_E(t;10,10,10)$. Figure 4A shows that for $0 < R < 15$ Å, $P_3(R)$ with $l = 10$ Å and $P_3^G(R)$ with $l_{EF} = 10.5$ Å exhibit a crude similarity in the distribution of end to end distances. Approximately 40% of the tagged chains lie within this range of both RDFs, consistent with the drop in $G^s(t)$ from 1.0 to 0.78.

$G^s(t)$ curves calculated with the degenerate exact and Gaussian RDFs for polymer chains with four statistical segments are presented in Figure 5B. $R_0 = 20$ Å. Using an l_{EF} of 10 Å results in a $G^s(t)$ calculated with a Gaussian RDF which mimics $G^s_E(t;10,10,20)$. The agreement is best
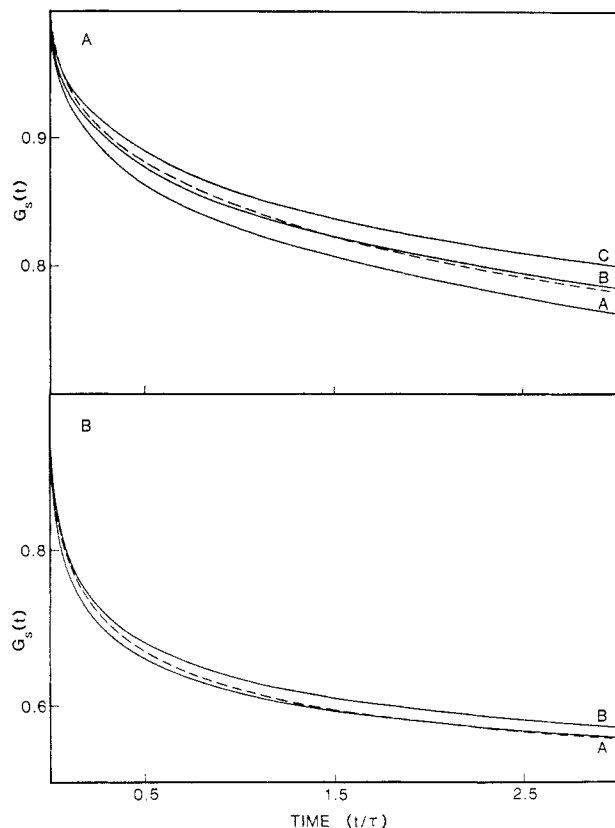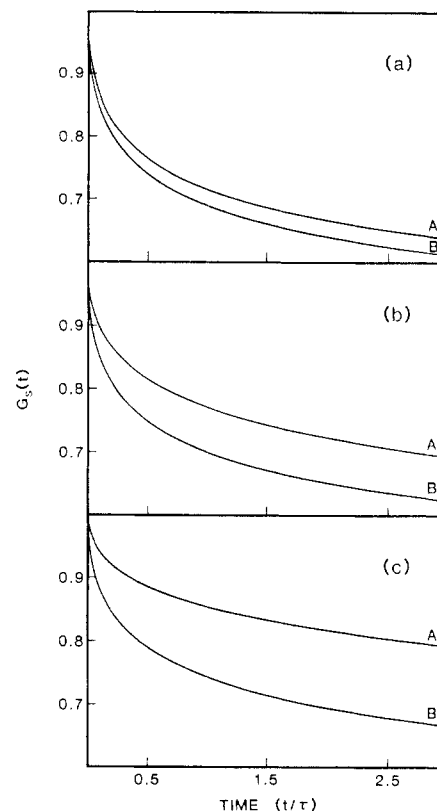
Figure 5. $G^s(t)$ calculated using the Gaussian and exact radial distribution functions. Calculations employing the Gaussian RDFs are shown as solid lines. See the text for an explanation of the $G^s(t)$ label notation. (A) An ensemble of three statistical segment polymers (RDFs displayed in Figure 4A) ($R_0 = 10$ Å): $G^s_E(t;-10,10,10)$ (——); $G^s_G(t)(t;10,10)$ (A); $G^s_G(t;10.5,10)$ (B); $G^s_G(t;11,10)$ (C). (B) An ensemble of four statistical segment polymers ($R_0 = 20$ Å); $G^s_E(t;10,10,20)$ (——); $G^s_G(t;10,20)$ (A); $G^s_G(t;10.5,20)$ (B).

Figure 6. $G^s(t)$ calculated for two models of end tagged polymer chains. The untagged polymer chain contains three 10-Å statistical segments. The tags either are incorporated into the terminal segments ($N = 3$) or are added as two additional statistical segments ($N = 5$). The exact radial distribution functions used in the calculations of $G^s(t)$ are shown in Figure 3. See the text for an explanation of the $G^s(t)$ label notation ($R_0 = 15$ Å): (a) $N = 3$, $G^s_E(t;11,10,15)$, (A); $N = 5$: $G^s_E(t;1,10,15)$, (B); (b) $N = 3$, $G^s_E(t;13,10,15)$, (A); $N = 5$: $G^s_E(t;3,10,15)$, (B); (c) $N = 3$, $G^s_E(t;17,10,15)$, (A); $N = 5$: $G^s_E(t;7,10,15)$, (B).

for $t > 0.5\tau$. At earlier times $G^s_G(t;10,20)$ decays faster than $G^s_E(t;10,10,20)$. $P_4{}^G(R)$ predicts that a greater fraction of the polymer chains will have end to end distances less than 15 Å than does $P_4(R)$. This leads to faster $G^s(t)$ decay for the Gaussian RDF at early times. Once chains with end to end distances greater than 15 Å begin to undergo substantial excitation transport, the differences between $G^s_E(t;10,10,20)$ and $G^s_G(t;10,20)$ diminish. $P_4(R)$ predicts a greater fraction of chains to have end to end distances between 15 and 30 Å than does $P_4{}^G(R)$. In the absence of lifetime effects, it is possible to see that $G^s_E(t,10,10,20)$ attains the value 0.5 prior to $G^s_G(t;10,20)$. Even for chains containing many statistical segments, the Gaussian RDF is much too large at end to end distances approaching and extending beyond the full chain extension.

Small differences between calculated $G^s(t)$ curves are readily interpreted in terms of differences in RDFs. However, noise in experimental data can be of the same order of magnitude as the small differences between calculated $G^s(t)$ curves for different RDFs (Figure 5, parts A and B). Comparisons between experimental and calculated $G^s(t)$ curves for a single chromophore pair may be insufficient to characterize the RDF of an ensemble of tagged chains. However, the calculations in Figure 5 suggest a method for more conclusive evaluation of proposed radial distribution functions. The correct RDF for an ensemble of tagged chains will reproduce the experimental $G^s(t)$ curves irrespective of the value of R_0. By performing a series of two or more experiments each using chains end-tagged with different chromophore pairs whose

R_0 span the range of distances available to the chain, one can test more stringently the accuracy of the proposed RDF. If the RDF statistical parameters that bring theoretical and experimental $G^s(t)$ curves into agreement must be altered when R_0 is altered, the proposed model is not an accurate representation of the chain end to end RDF. The correct RDF in eq 21 will reproduce experimentally determined $G^s(t)$ curves for different R_0's without recourse to changing the statistical parameters.

An alternative, and generally preferable, approach is to use a single chromophore pair with an R_0 comparable to the extended chain length. This method can provide a probe of the short R portions of the RDF if measurements are made from short time scales to long time scales, since chains with $R < R_0/2$ undergo transport and depolarization of the excitation prior to 0.01τ. Since the typical lifetimes of chromophores range from 10 nsec to 100 ns, the short time requirement implies measurements on the time scale of 100 ps to 1.0 ns. These are easily accessible time scales with straightforward commercial equipment.

Figure 6 presents calculated $G^s(t)$ curves for the three- and five-step RDF models of end-tagged polymer chains shown in Figure 3. R_0 for these calculations is 15 Å, one half the extended length of the untagged polymer chain. In each case, $G^s(t)$ derived from the five-step model decays faster. Longer connections between the chromophores and polymer chain termini increase the disparity between $G^s(t)$ calculated with the two models. It is clear that the length and flexibility of the tags employed to investigate polymer RDFs can have very dramatic effects on both the exper-

imental observation and on the manner in which the data are interpreted. The differences between the RDFs and $G^s(t)$s calculated with the above two models for end-tagged polymer chains can be comparable to the differences produced by using exact of Gaussian radial distribution functions. In order to obtain meaningful characterization of polymer radial distribution functions from end to end energy transport studies, the end tags and the models used to incorporate them into the chain statistics must be carefully chosen.

V. Conclusion

Sophisticated models exist which include atomic and molecular level interactions in calculations of the statistical properties of polymer chains.[15] These methods can provide end to end radial distribution functions for short oligomers; the rapidly increasing number of degrees of freedom make calculations for short polymer chains prohibitive. Thus, theoretical models of radial distribution functions must use coarse grain representations,[16] i.e., the detailed interactions between neighboring groups are absorbed into a less detailed, more macroscopic picture of the chain. The Kuhn equivalent chain,[3] in which a string of monomers, termed a statistical segment, is replaced by a single rigid step in a freely jointed chain (random walk), is the simplest of such models. In the limit of an infinitely long chain, the Kuhn chain radial distribution function attains a Gaussian form. Gaussian RDFs are adequate models for long and moderate length flexible polymer chains. For short chains, containing a few statistical segments, the freely jointed chain RDF and the Gaussian RDF are different.

Radial distribution functions cannot be directly determined experimentally. Instead, measurements are made on a distance dependent observable which can be related to a chain statistical property, for example, the end to end distance. Information concerning the RDF is convolved with the distance dependence of the observable. This process tends to blur the details of the RDF shape. As a consequence, the coarse grain representations of polymer RDFs may be sufficient for use in the majority of experimental investigations.

Fluorescence and absorption depolarization techniques are frequently used to investigate the properties of polymer systems.[9a,17] Electronic excitation transport can contribute significantly to depolarization in chains with more than one chromophore. The rate of excitation transport depends on $1/R^6$. Thus, measurements of time-dependent depolarization in chromophore end tagged chains can be used to investigate polymer end to end radial distribution functions.

The relevant quantity in such experiments is the chromophore to chromophore RDF, which differs from the untagged chain end to end RDF. In order to explicitly and more realistically include in the RDF the additional distance introduced by the tags, we have derived formulas for the exact end to end radial distribution function of a freely jointed chain in which each chain segment can be of any length. This model can be applied to tagged chains by using two statistical segment lengths; one corresponding to the internal unperturbed statistical segments of the polymer and a second that represents the chain ends plus tag. We have used the exact two segment length RDF, a single segment length RDF and a Gaussian RDF to calculate the ensemble averaged time dependence of electronic excitation transport in polymer chains with identical chromophores at the two termini. These calculations lead us to conclude the following:

(i) Electronic excitation transport studies can be used

to investigate the details of polymer chain radial distribution functions. Determination of the correct RDF form is most confidently achieved by making measurements on a series of polymers, end tagged with chromophore pairs with critical transfer radii, R_0, which span the end to end distances accessible to the chain. The RDF statistical parameters employed to simulate the excitation transport observable will be independent of R_0 for the correct RDF. Alternatively, observing excitation transport between end tags with R_0 comparable to the extended length of the polymer over a wide range of time scales can provide a stringent test of the RDF. An accurate RDF will reproduce the full time dependence of the experiment. It may be possible to aid the analysis by using detailed conformational calculations on short sections of chains as inputs for the statistical segment lengths and for the tag structures. Such calculation could also provide probability distributions for the variations in the segment lengths. These could be used with the general formulas provided in section II, to perform averages over the segment size for each step in the walk.

(ii) The choices of tags employed and their incorporation into the polymer chain model are important. The addition of large or excessively flexible end groups can introduce as much uncertainty into the modeling of the chain statistics as does the form of the radial distribution function. However, knowledge of the molecular structure of the tag can remove some of the uncertainty. Very flexible end tags are probably best modeled as independent segments, while rigid tags should probably be included as parts of the chain terminal segments.

(iii) Gaussian and exact RDFs can be made brought into congruence over limited end to end distance ranges of the polymer chain by employing slightly modified statistical parameters. Calculated observables, dependent on the RDF only within this distance range, will appear very similar. If approximate statistical parameters, and not RDF details, are of interest, either RDF form may be employed. For example, studies of changes in polymer chain dimensions in miscible versus immiscible blends may be adequately pursued by using either form of the RDF.

Electronic excitation transport studies can provide characterization of polymer properties. Judicious choices of chromophore pairs, tag structure, and chain models will extend the accuracy and the utility of the experimental conclusions. While the distribution functions presented in eq 18 and 19 have been illustrated with calculations of the excitation transport observable, these distribution functions can be employed to calculate other observables, such as X-ray scattering from bromine end tags, which may be capable of providing more detailed insights into short chain end to end distribution functions.

References and Notes

(1) Jernigan, R. L.; Flory, P. J. *J. Chem. Phys.* **1969**, *50*, 4185.
(2) Chandresekhar, S. *Rev. Mod. Phys.* **1943**, *15*, 1.
(3) Kuhn, W.; Kuhn, H. *Helv. Chim. Acta* **1943**, *26*, 1394.
(4) Lord Rayleigh, *Philos. Mag. S.* **1919**, *37*, 321.
(5) Jernigan, R. L.; Flory, P. J. *J. Chem. Phys.* **1969**, *50*, 4165.
(6) (a) Ediger, M. D.; Fayer, M. D. *Macromolecules* **1983**, *16*, 1839. (b) Frederickson, G. H.; Andersen, H. C.; Frank, C. W. *J. Polym. Sci., Polym. Phys. Ed.* **1985**, *23*, 591. (c) Peterson, K. A.; Fayer, M. D. *J. Chem. Phys.* **1986**, *85*, 4702.

(7) *Photophysics of Polymers*; Hoyle, C., Torkelson, J., Eds.; ACS Symposium Series 358; American Chemical Society: Washington, DC, 1987.

(8) (a) Gochanour, C. R.; Andersen, H. C.; Fayer, M. D. *J. Chem. Phys.* **1979**, *70*, 4524. (b) Loring, R. F.; Andersen, H. C.; Fayer, M. D. *J. Chem. Phys.* **1982**, *76*, 2015.

(9) (a) Peterson, K. A.; Zimmt, M. B.; Linse, S.; Domingue, R. P.; Fayer, M. D. *Macromolecules* **1987**, *20*, 168. (b) Ediger, M. D.; Domingue, R. P.; Peterson, K. A.; Fayer, M. D. *Macromolecules* **1985**, *18*, 1182. (c) Ediger, M. D.; Domingue, R. P.; Fayer, M. D. *J. Chem. Phys.* **1984**, *80*, 1246.

(10) Förster, Th. *Ann. Phys.* **1948**, *2*, 55.

(11) Barber, M. N.; Ninham, B. W. *Random and Restricted Walks: Theory and Applications*; Gordon and Breach: New York, 1970.

(12) A four-segment model, with two unperturbed internal segments and two terminal, tag plus polymer segments, can also be used. The behavior is intermediate between the $N = 3$ and $N = 5$ results.

(13) (a) Gochanour, C. R.; Fayer, M. D. *J. Phys. Chem.* **1981**, *85*, 1989. (b) Steinberg, I. Z. *J. Chem. Phys.* **1968**, *48*, 2411. (c) Blumen, A. *Ibid.* **1981**, *74*, 6926.

(14) Galanin, M. D. *Tf. Fiz. Inst. I. P. Pavlova* **1950**, *5*, 341.

(15) (a) Volkenstein, M. V. *Configurational Statistics of Polymeric Chains*; Wiley-Interscience: New York, 1963. (b) Flory, P. J. *Statistical Mechanics of Chain Molecules*; Wiley-Interscience: New York, 1969.

(16) (a) de Gennes, P. G. *Scaling Concepts in Polymer Physics*; Cornell University Press: Ithaca, NY, 1979. (b) Freed, K. F. *Renormalization Group Theory of Macromolecules*; Wiley: New York, 1987.

(17) (a) Viovy, J.-L.; Monnerie, L.; Merola, F. *Macromolecules* **1985**, *18*, 1130. (b) Hyde, P. D.; Waldow, D. A.; Ediger, M. D.; Kitano, T.; Ito, K. *Macromolecules* **1986**, *19*, 2533.